Noise-enhanced temporal association in neural networks

Y. Shim, H. Hong, and M. Y. Choi
Department of Physics and Center for Theoretical Physics, Seoul National University, Seoul 151-747, Korea
(Received 7 August 2001; revised manuscript received 2 November 2001; published 12 February 2002)

We consider a network of globally coupled neuronal oscillators subject to random force, and investigate numerically dynamic responses to external periodic driving. The order parameter, which measures the overlap between the configuration of the system and embedded patterns, is found to exhibit stochastic resonance behavior, as manifested by the signal-to-noise ratio (SNR). The optimal noise level at which the SNR reaches its maximum is found to depend on the driving frequency. On the other hand, as the randomness in the driving amplitude is increased, the system undergoes a transition from the memory-retrieval state to the mixed-memory one. The noise effects on the temporal-association state in the absence of external periodic driving are also investigated, revealing similar noise-enhanced resonance.

DOI: 10.1103/PhysRevE.65.036114 PACS number(s): 84.35.+i, 05.45.Xt, 87.18.Sn, 05.40.−a

I. INTRODUCTION

Dynamics of the systems consisting of a large number of coupled nonlinear oscillators is an intriguing subject in physics, chemistry, biology, and social sciences [1]. In particular, those systems have been shown to exhibit the remarkable phenomena of *collective synchronization* [2], which have been observed in various systems including charge-density waves, laser, Josephson-junction arrays, chemical reactions, and biological systems such as neural networks [3–6]. Recently, collective synchronization in the neural network has been studied by regarding each neuron as a limit-cycle oscillator and modeling the system as a set of coupled neuronal oscillators [7,8]. The limit-cycle model conveniently describes oscillatory behavior and naturally exhibits synchronization as a mechanism for the storage of memory. In a previous study [9], the collective synchronization behavior has been investigated in terms of the limit-cycle oscillator model, with attention to the interplay of the symmetric coupling and the asymmetric one. Particularly, in that study, the temporal-association state that arises by the interplay between the two couplings has been reported, and the phase boundaries separating the memory-retrieval state, the mixed-memory state, the no-memory state, and the temporal-association state have been numerically obtained on the plane of the asymmetry-to-symmetry ratio and the coupling strength. Meanwhile, the noise effects on the temporal-association state have not been explored in Ref. [9]. In general, a macroscopic system with many degrees of freedom is necessarily coupled to the environment, and accordingly noise is unavoidable. Further, in view of that biological systems are open and subject to the external driving, often periodic in time, the effects of external driving are also relevant and to be investigated [10]. In particular, the presence of both external driving and noise raises the interesting possibility that the interplay between the two may give rise to resonance behavior [11].

In this paper, we consider a network of globally coupled neuronal oscillators subject to random force, and investigate numerically dynamic responses to external periodic driving. Performing simulations with various values of the parameters, we examine how successful memory retrieval is realized under external driving and noise, probe the noise effects on the memory-retrieval state, and obtain how the phase boundary between the memory-retrieval state and the mixed-memory one varies on the plane of the frequency and randomness of the driving. The order parameter, which measures the overlap between the configuration of the system and embedded patterns, is found to exhibit stochastic resonance behavior, as manifested by the signal-to-noise ratio (SNR) [12]. The optimal noise level at which the SNR reaches its maximum is observed to depend on the driving frequency. On the other hand, as the randomness in the driving amplitude is increased, the system undergoes a transition from the memory-retrieval state to the mixed-memory one. The noise effects on the temporal-association state in the absence of external periodic driving are also investigated, revealing noise-enhanced resonance behavior.

There are four sections in this paper. Section II introduces the driven system of coupled neuronal oscillators, and investigates the effects of noise and periodic driving on the memory-retrieval state. In Sec. III noise effects on the temporal-association state are examined. In addition, stochastic resonance behavior is also explored in the presence of external periodic driving. Finally, a brief summary is given in Sec. IV.

II. DRIVEN SYSTEM OF NEURONAL OSCILLATORS

We begin with the set of equations of motion governing the dynamics of N coupled neurons, the state of the ith of which is described by the phase ϕ_i $(i=1,2,\ldots,N)$

$$\frac{d\phi_i}{dt}=\omega_i-\sum_{j=1}^{N} J_{ij}\sin(\phi_i-\phi_j)+I_i\cos\Omega t+\Gamma_i(t). \quad (1)$$

The intrinsic frequency ω_i of the ith oscillator is randomly distributed over the whole system, according to the Gaussian distribution with zero mean $(\overline{\omega}=0)$ and variance σ_ω. The second term on the right-hand side denotes the coupling between the neurons, and the third one represents external periodic driving. The driving frequency Ω is assumed to be uniform for all oscillators, whereas the driving strength I_i is allowed to vary for different oscillators. For simplicity, I_i's are assumed to be randomly distributed according to the

Gaussian distribution with variance σ_I and zero mean ($\bar{I}=0$). The last term corresponds to the white noise with zero mean and correlation $\langle \Gamma_i(t)\Gamma_j(t')\rangle = 2T\delta_{ij}\delta(t-t')$, where the noise strength T plays the role of the *effective temperature* of the system. When the coupling is uniform ($J_{ij}=K/N$) and the external periodic driving is absent ($I_i=0$), Eq. (1) reduces to the simple oscillator model studied extensively [2]. In biological neural networks, on the other hand, synaptic connections are neither uniform nor symmetric, taking into account memory storage according to Hebb's hypothesis. In view of this, we here consider the synaptic coupling in the form

$$J_{ij} = J_{ij}^s + \lambda J_{ij}^a, \tag{2}$$

where the symmetric component J_{ij}^s and the asymmetric one J_{ij}^a are given by

$$J_{ij}^s = \frac{2K}{N}\sum_{\mu=1}^{p}\cos(\xi_i^\mu - \xi_j^\mu),$$

$$J_{ij}^a = \frac{2K}{N}\sum_{\mu=1}^{p}\cos(\xi_i^\mu - \xi_j^{\mu-1}) \tag{3}$$

with λ controlling the relative strength of the asymmetric component. This assignment corresponds to that p patterns are stored in the system. The μth stored pattern ($\mu=1,2,\ldots,p$) is given by the set $\{\xi_i^\mu | i=1,\ldots,N\}$, where ξ_i^μ represents the state (phase) of the ith neuron (in the μth pattern) and is assumed to be distributed randomly in the interval $[0,2\pi)$. For the asymmetric component, which mimics the high degree of asymmetry in the biological synaptic connections, cyclic boundary conditions $\xi_i^0 \equiv \xi_i^p$ have been taken. Such asymmetric coupling of the type given by Eq. (3) has been studied in models of neural networks, and successive retrieval of a sequence of embedded patterns has been demonstrated [9,13].

Collective synchronization of the system is conveniently described by the set of complex order parameters

$$\Psi^\mu \equiv \frac{1}{N}\sum_{j=1}^{N} e^{i(\phi_j \pm \xi_j^\mu)} \equiv \Delta_\pm^\mu e^{i\theta_\pm^\mu}, \tag{4}$$

where Δ_-^μ measures the overlap between the state of the network and the μth pattern ξ^μ. Thus nonzero values of Δ_-^μ signals the appearance of synchronization and plays the role of the order parameter while Δ_+^μ is an auxiliary order parameter. Using the set of order parameters defined in Eq. (4) together with Eq. (3), we decouple the set of dynamic equations (1) and obtain the single-neuron equation

$$\begin{aligned}\frac{d\phi_i}{dt} = {} & \omega_i + I_i\cos\Omega t + \Gamma_i(t) - K\sum_{\mu=1}^{p}[\Delta_-^\mu \sin(\phi_i - \theta_-^\mu - \xi_i^\mu) \\ & + \Delta_+^\mu \sin(\phi_i - \theta_+^\mu + \xi_i^\mu)] \\ & - \lambda K\sum_{\mu=1}^{p}[\Delta_-^{\mu-1}\sin(\phi_i - \theta_-^{\mu-1} - \xi_i^\mu) \\ & + \Delta_+^{\mu-1}\sin(\phi_i - \theta_+^{\mu-1} + \xi_i^\mu)],\end{aligned} \tag{5}$$

where $\Delta_\pm^\mu$ are to be determined by imposing self-consistency.

In the simplest case that the asymmetric coupling, external driving, and noise are all absent ($\lambda = I_i = T = 0$), the system can indeed be in the memory-retrieval state characterized by the emergence of collective synchronization, i.e., a nonzero value of $\Delta_-^\mu \equiv \Delta^\mu$ for some μ [7,8]. When the number of patterns p stored in the network is small, i.e., the storage $\alpha \equiv p/N$ is less than the capacity α_c, the Mattis state, which possesses a nonvanishing overlap with only a single pattern, say $\mu=1$, is globally stable and the transition between the memory-retrieval state and the no-memory one, where all components of the order parameter vanishes corresponds to simply the synchronization-desynchronization transition.

To examine the role of external driving in memory retrieval, we have performed numerical simulations on Eq. (5), in the absence of the asymmetric coupling and noise ($\lambda = T = 0$). Throughout this work, unless specified otherwise, the coupling strength and the variance of the natural frequency distribution are set to be $K=10$ and $\sigma_\omega = 1.0$, respectively, which guarantees the memory-retrieval state in the absence of external driving. We integrate Eq. (5) via the Euler method with discrete time steps of $\Delta t = 0.016$ and compute the order parameter given by Eq. (4) using $N_t = 60\,000$ time steps at each run, with the data from the first 1024 steps discarded. Ten independent runs with different initial configurations have been performed over which averages have been taken.

Figure 1(a) shows the time evolution of the order parameter Δ^μ obtained in the network of $N=2048$ oscillators with $p=10$ random stored patterns. The network is driven periodically with the frequency $\Omega=\pi$ and the variance of the amplitude distribution $\sigma_I = 0.5$. It is shown that the system is in the memory-retrieval state even in the presence of random periodic driving. It is also observed that the periodic driving generates an oscillation of the order parameter with the same frequency [see the inset of Fig. 1(a)]. As the randomness of the driving amplitude, measured by the variance σ_I, is raised, the largest component of the order parameter tends to diminish while other ones grow. Eventually, when σ_I exceeds the critical variance $\sigma_{Ic} \approx 3.6$, the memory-retrieval state no longer persists and the mixed-memory state possessing overlaps with two or more patterns appears, as shown in Fig. 1(b). This is to be contrasted with the undriven system (with $\lambda = T = 0$) which exhibits only the memory-retrieval state for $\alpha < \alpha_c$. It is thus concluded that periodic driving with sufficiently strong randomness can give rise to the mixed-memory state at zero temperature. Note the difference from the mixed-memory state generated by the nonzero asymmetric coupling ($\lambda \neq 0$) in the undriven system, which possesses the same nonvanishing overlap with all the stored patterns [9].

Performing simulations on the system with various values of the parameters Ω, σ_I, and p, we have obtained the phase boundary between the memory-retrieval state and the mixed-memory one on the plane of (Ω, σ_I), which is shown in Fig. 2. As σ_I is raised from zero, the component $\Delta^{\mu=1}$ corre-

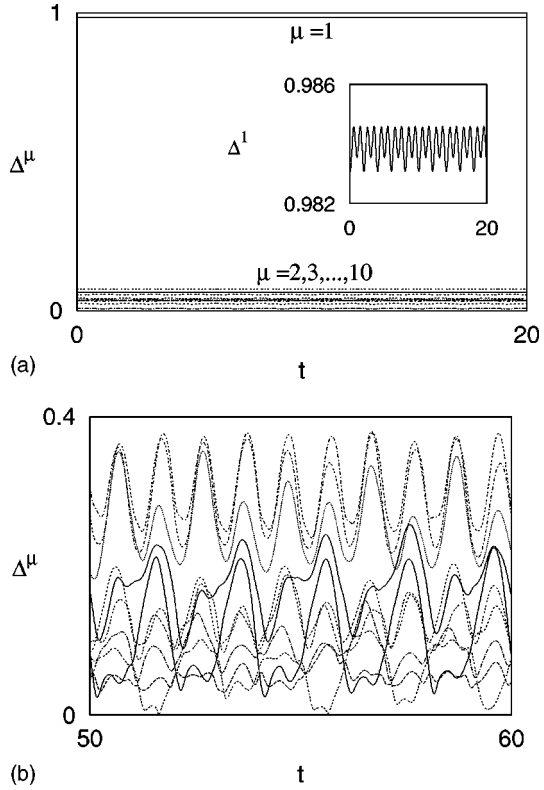

FIG. 1. Behavior of the order parameter with time (a) in the memory-retrieval state and (b) in the mixed-memory state of the driven system without asymmetric coupling and noise ($\lambda = T = 0$). In (a) the uppermost curve near unity corresponds to Δ^1 while other components ($\mu \neq 1$) are shown to be negligible. The detailed behavior of Δ^1 during the same time interval is shown in inset, revealing the periodic motion with the driving frequency $\Omega = \pi$. Simulations have been performed on the system of $N = 2048$ oscillators with $p = 10$ stored patterns and the variance of the natural frequency distribution $\sigma_\omega = 1.0$. The variance of the driving amplitude distribution is given by $\sigma_I = 0.5$ in (a) and 6.0 in (b).

sponding to the retrieved pattern, decreases from unity while other components ($\mu \neq 1$) in general grow from zero. The critical value σ_{Ic} or the phase boundary in Fig. 2 has been determined according to the condition that Δ^1 becomes equal to Δ^μ for some $\mu \neq 1$. It is observed that σ_{Ic} increases monotonically with the external driving frequency Ω. Note also that larger values of p (for given size $N = 2048$) correspond to larger values of the storage α and result in smaller values of σ_{Ic}, suggesting that large storage tends to suppress single memory retrieval. To check possible finite-size effects, we have considered systems of various sizes and number of stored patterns at given values of the storage α. For example, we have considered the system with $(N,p) = (1024,4)$ and obtained the phase boundary fully coincident with that for $(N,p) = (2048,8)$. This indicates both that finite-size effects are not substantial for $N \gtrsim 1024$ and that the phase boundary depends upon the storage α. As σ_I is increased further to a value sufficiently larger than σ_{Ic}, the mixed-memory state is finally replaced by the no-memory state. Namely, driving with very strongly random amplitudes eventually destroys synchronization completely. In addition, we have also

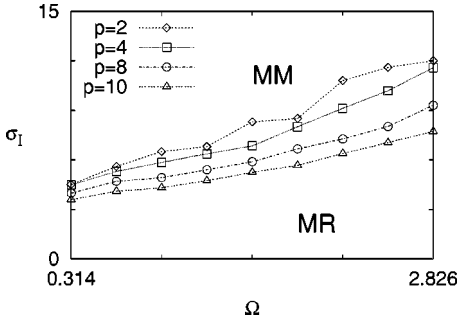

FIG. 2. Schematic phase boundary on the plane of the driving frequency Ω and the variance of the driving amplitude distribution σ_I. The boundary separating the memory-retrieval state (MR) from the mixed-memory state (MM) is displayed for various p the numbers of stored patterns. Error bars estimated by the standard deviation have about the same sizes as those of the symbols, and lines are merely guides to the eyes.

checked how robust the phase boundary is against noise, and found that it persists in the presence of moderate amounts of noise. When the noise grows sufficiently strong, however, coherence is again destroyed, leading to the no-memory state.

III. STOCHASTIC RESONANCE IN TEMPORAL ASSOCIATION

In this section, we consider both the symmetric coupling and the asymmetric one in Eq. (5); the presence of both the two couplings has been known to give the temporal-association state in appropriate regions of the parameter space [9]. We first examine how the random noise affects the temporal-association state in the absence of external periodic driving ($I_i = 0$). For this purpose, we have performed extensive numerical simulations on Eq. (5), varying the noise strength T. The asymmetric ratio has been set to be $\lambda = 0.4$, which, together with the coupling strength $K = 10$ and the variance of the intrinsic frequency distribution $\sigma_\omega = 1.0$, again yields the temporal-association state in the absence of random noise [9]. Equation (5) for the system of $N = 5000$ oscillators has been integrated via the same method as that used in Sec. II. In computing the order parameter, $N_t = 6 \times 10^4$ time steps have been used at each run, with the data from the first 3.6×10^3 steps discarded. Twelve independent runs with different initial configurations have been performed, over which averages have been taken.

Figure 3(a) shows the obtained temporal behavior of the order-parameter component Δ^1 corresponding to the retrieved pattern at various noise levels $T = 0.0$, 0.5, 1.0, and 1.5. It is observed that the period of the oscillations of the order parameter in the temporal-association state decreases as the noise strength is increased. To make this clear, we have computed the power spectrum of the component Δ^1,

$$P(\omega) \equiv \langle |\tilde{\Delta}^1(\omega)|^2 \rangle, \tag{6}$$

where $\tilde{\Delta}^1(\omega) \equiv (1/2\pi) \int dt \Delta^1(t) e^{i\omega t}$ is the Fourier component of Δ^1 at frequency ω and $\langle \cdots \rangle$ represents the ensemble

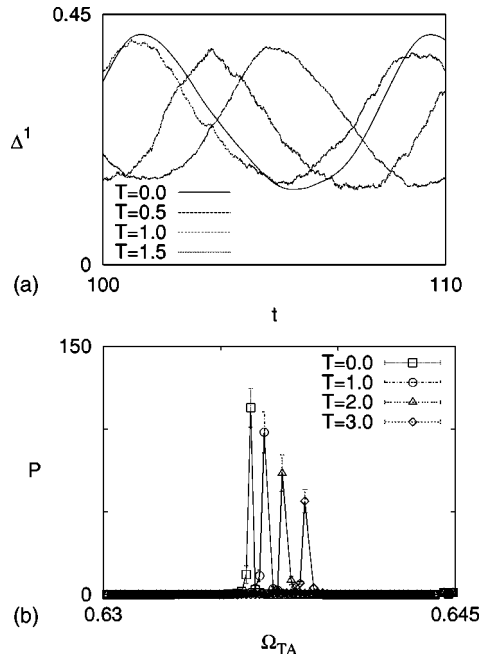

FIG. 3. (a) Temporal behavior of the order parameter for the retrieved pattern at noise strength $T=0.0$, 0. 5, 1. 0, and 1. 5, in the undriven system of $N=5000$ oscillators with $\lambda=0.4$ and $p=10$. (b) Corresponding power spectrum of the order parameter (in arbitrary units), displaying sharp peaks at frequency $\omega=0.6366$, 0.6372, 0.6379, and 0.6389 for noise strength $T=0.0$, 1.0, 2.0, and 3.0, respectively. Error bars have been estimated by the standard deviation and lines are guides to the eye.

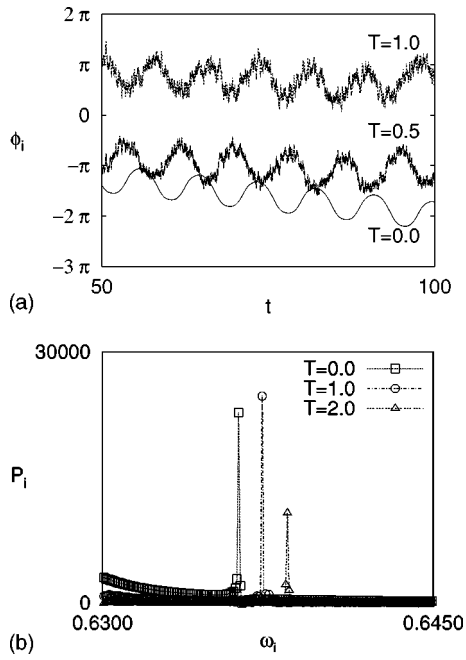

FIG. 4. (a) Time evolution of the phase ϕ_i of an arbitrarily chosen oscillator at noise strength $T=0.0$, 0.5, and 1.0, in the system of Fig. 3. For clarity, the data for $T=1.0$ have been lifted upward by $3\pi/2$. (b) Corresponding power spectrum of the phase (in arbitrary units), displaying sharp peaks at the same frequency as Fig. 3(b) for noise strength $T=0.0$, 1.0, and 2.0.

average. As shown in Fig. 3(b), a sharp peak develops at a nonzero frequency, which tends to shift toward higher frequencies as the noise strength is increased. With regard to this, we also examine how the phase of each oscillator evolves with time. In the memory-retrieval state, the phase has been observed to evolve monotonically with time. In contrast, Fig. 4 reveals that in the temporal-association state the phase has an oscillating component, with the same frequency as the order parameter in Fig. 3. This behavior may be understood in the following way: Equation (5) may be considered to describe the motion of an overdamped particle in the appropriate potential well with p minima corresponding to p embedded patterns. The barrier between minima is proportional to both the coupling strength and the magnitude of the order parameter Δ^{μ}, which in turn depends on the noise strength. Consequently, the barrier height decreases with the noise level, resulting in higher frequency of the interwell motion of the particle, i.e., higher frequency of the time evolution of phase ϕ_i [see Fig. 4(b)]. Such interwell motion between successive minima eventually leads to the oscillation of the order-parameter component; it is thus concluded that noise in general increases the frequency of the order-parameter oscillation or of the power spectrum peak.

For more detailed examination of the noise effects on temporal association, we also consider the SNR, $\mathcal{R}$ defined to be

$$\mathcal{R}\equiv\ln\left[\frac{S}{N}\right], \tag{7}$$

where signal S and noise N are given by the peak value of the power spectrum in Eq. (6) and its background noise, respectively. The background noise N at the frequency of the peak has been estimated from the intrapolation of the power spectrum data around the peak. Since there does not exist the characteristic (driving) frequency in the undriven system considered at present, we compute the SNR at various frequencies and plot in Fig. 5 its behavior with the noise level T. Observed is the optimal noise level at which the SNR at given frequency reaches its maximum; thus manifested is the noise-enhanced resonance without external periodic driving [14]. The five sets of data exhibiting such resonance behavior in Fig. 5 describe the SNR at frequencies $\omega=0.6368$, 0.6372, 0.6376, 0.6379, and 0.6383, respectively. It is shown that the optimal noise level at which the SNR reaches its maximum increases with the frequency, reflecting the shift of the power spectrum peak in Fig. 3(b). Note also that the peak value of the SNR (regardless of the frequency) at given noise level appears to decrease monotonically as the noise level is raised. When the noise level is increased beyond $T_c\approx 5$, the temporal-association state no longer persists, thus making the noise-enhanced resonance behavior unobservable.

The behavior of the SNR has also been investigated for various coupling strengths. For given coupling strength, we have computed the SNR at the frequency ω_m, which yields the highest peak of the power spectrum in the range $0\leqslant T\leqslant 0.9$. Figure 6 displays the obtained behavior at the frequency ω_m, which turns out to be $\omega_m=0.6333$, 0.6368, and 0.6402 for the coupling strengths $K=5$, 10, and 15, respectively. It is found that both the optimal noise level and the

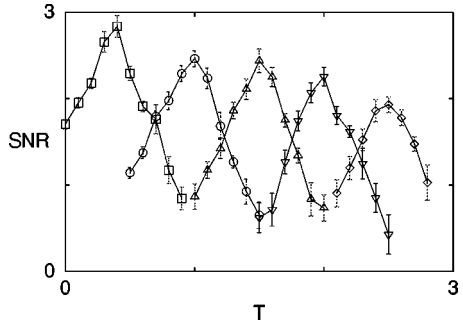

FIG. 5. Behavior of the signal-to-noise ratio (SNR) with the noise level T in the temporal-association state of the system in Fig. 3, exhibiting noise-enhanced resonance. Five sets of data correspond to the frequency $\omega=0.6368$ ($\square$), 0.6372 ($\bigcirc$), 0.6376 ($\triangle$), 0.6379 ($\triangledown$), and 0.6383 ($\diamond$), respectively. Error bars have been estimated by the standard deviation and lines are again guides to the eye.

frequency ω_m yielding the highest peak for given coupling strength in general increase with the coupling strength.

We now turn on external periodic driving and examine the interplay between the driving and noise in the temporal-association state. The variance of the distribution of the driving amplitude is chosen to be $\sigma_I=1.0$ for convenience, while the values of other parameters are set equal to those in the undriven system. To explore the effects of external periodic driving on temporal association, we consider various driving frequencies and compute the SNR in each driven system. The SNR at the driving frequency, i.e., at $\omega=\Omega$, versus the noise level is shown in Fig. 7 for driving frequency (a) $\Omega=0.6368$; (b) $\Omega=0.6372$; (c) $\Omega=0.6376$. The obtained data represented by boxes manifest the presence of the SNR peak and the corresponding optimal noise level at each driving frequency, thus revealing stochastic resonance phenomena. For comparison, also displayed [represented by triangles in (a), (b), and (c)] is the SNR at the same frequency $\omega=0.6368$, 0.6372, and 0.6376, respectively, in the undriven system, which has already been shown in Fig. 5. Note that the optimal noise level is reduced in the presence of periodic driving. Namely, external driving lowers the noise level necessary for achieving the maximal SNR. Except for the position of the peak, however, the two sets of data in Fig. 7 display qualitatively similar behavior, suggesting no essential difference in the noise-induced resonance regardless of the presence of external driving.

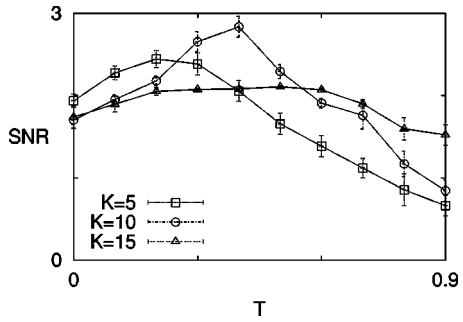

FIG. 6. SNR versus the noise level T at various coupling strengths in the temporal-association state of the undriven system, with other parameters the same as those in Fig. 3. The data for the coupling strength $K=5$, 10, and 15 represent the SNR at frequency $\omega=0.6333$, 0.6368, and 0.6402, respectively.

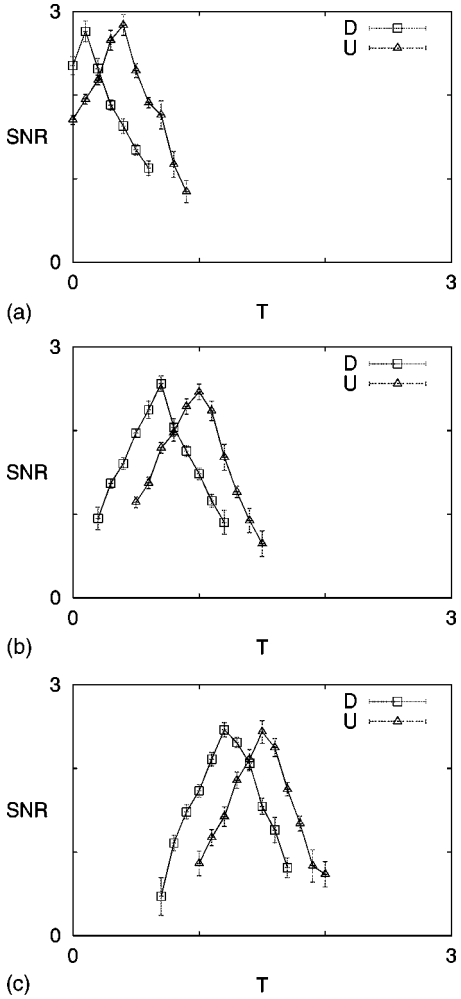

FIG. 7. Comparison of the behavior of the SNR at frequency (a) $\omega=0.6368$, (b) $\omega=0.6372$, and (c) $\omega=0.6376$ in the driven system (D) and in the undriven system (U). In the driven system the SNR has been computed at the driving frequency Ω, i.e., $\omega=\Omega$.

To see this, we also examine the SNR at frequency ω different from the driving frequency. Figure 8 shows the obtained SNR at frequency $\omega=0.6368$ versus the noise level in the system with driving frequency $\Omega=0.6283$, 1.2566, 3.1416, and 6.2832. It is observed that the resonance behavior in the driven system indeed exists at given frequency, regardless of the driving frequency. In other words, the system driven with given frequency displays resonance peaks in the SNR at various frequencies, similarly to the undriven system shown in Fig. 5. It is also shown in Fig. 8 that the optimal noise level for the SNR at given frequency in general increases with the driving frequency.

IV. SUMMARY

We have considered a network of globally coupled neuronal oscillators subject to random force, and investigated numerically dynamic responses to external periodic driving.

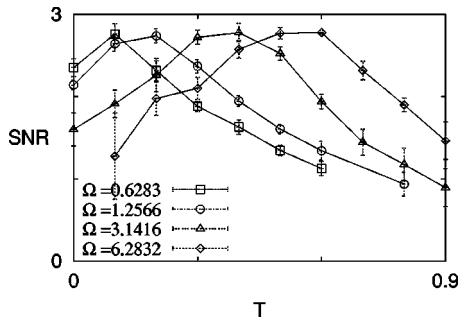

FIG. 8. SNR at frequency $\omega = 0.6368$ versus the noise level T in the driven system with driving frequency Ω and other parameters the same as those in Fig. 3.

By means of simulations with various values of the parameters, we have examined memory retrieval under external driving and noise, with attention to the noise effects on the temporal-association state. The phase boundary between the memory-retrieval state and the mixed-memory one has been obtained on the plane of the frequency and randomness of the driving. The order parameter, which measures the overlap between the configuration of the system and embedded patterns, has been found to exhibit noise-induced resonance, as manifested by the SNR. Here two kinds of the noise effects are present: One is the enhancement of the response, which is the mechanism for the conventional stochastic resonance, and the other is the shift of the power spectrum peak toward high frequencies. To our knowledge, the latter, which results from the decrease of the barrier height in the presence of noise, has not been reported in previous studies. In particular, no qualitative difference in the resonance behavior has been observed between the driven system and the undriven one. Thus high driving frequency increases the optimal noise level, whereas large randomness in the driving amplitude eventually drives the transition to the mixed-memory state. The detailed understanding of these behaviors and their implications to applicable biophysical systems requires more extensive investigations, which are left for further study.

ACKNOWLEDGMENT

This work was supported in part by the Ministry of Education through the BK21 Program.

[1] For a list of references, see, e.g., A.T. Winfree, *The Geometry of Biological Time* (Springer-Verlag, New York, 1980); Y. Kuramoto, *Chemical Oscillations, Waves, and Turbulence* (Springer-Verlag, Berlin, 1984); L. Glass and M.C. Mackey, *From Clocks to Chaos: The Rhythm of Life* (Princeton University Press, Princeton, 1988).

[2] Y. Kuramoto and I. Nishikawa, J. Stat. Phys. **49**, 569 (1987); H. Daido, Prog. Theor. Phys. **77**, 622 (1987); Phys. Rev. Lett. **68**, 1073 (1992).

[3] S.P. Benz, M.S. Rzchowski, M. Tinkham, and C.J. Lobb, Phys. Rev. Lett. **64**, 693 (1990); M.Y. Choi, Phys. Rev. B **46**, 564 (1992); S. Kim, B.J. Kim, and M.Y. Choi, *ibid.* **52**, 13 536 (1995); K. Wiesenfeld and J.W. Swift, Phys. Rev. E **51**, 1020 (1995); K. Park and M.Y. Choi, Phys. Rev. B **56**, 387 (1997).

[4] L. Fabiny, P. Colet, R. Roy, and D. Lenstra, Phys. Rev. A **47**, 4287 (1993); J.F. Heagy, T.L. Caroll, and L.M. Pecora, Phys. Rev. E **50**, 1874 (1994); R. Roy and K.S. Thornburg, Jr., Phys. Rev. Lett. **72**, 2009 (1994).

[5] T.J. Walker, Science **166**, 891 (1969); D.C. Michaels, E.P. Maytyas, and J. Jalife, Circ. Res. **61**, 704 (1987); R.D. Traub, R. Miles, and R.K.S. Wong, Science **243**, 1319 (1989).

[6] R. Eckhorn, R. Bauer, W. Jordan, M. Brosch, W. Kruse, M. Munk, and R.J. Reitboeck, Biol. Cybern. **60**, 121 (1988); C.M. Gray and W. Singer, Proc. Natl. Acad. Sci. U.S.A. **86**, 1698 (1989).

[7] A. Arenas and C.J.P. Vicente, Europhys. Lett. **26**, 79 (1994).

[8] K. Park and M.Y. Choi, Phys. Rev. E **52**, 2907 (1995).

[9] H. Hong, T.I. Um, Y. Shim, and M.Y. Choi, J. Phys. A **34**, 5021 (2001).

[10] M.Y. Choi, Y.W. Kim, and D.C. Hong, Phys. Rev. E **49**, 3825 (1994); M.Y. Choi, in *Neural Networks: The Statistical Mechanics Perspectives*, edited by J.-H. Oh, C. Kwon, and S. Cho (World Scientific, Singapore, 1995), pp. 156–166.

[11] H. Hong, M.Y. Choi, K. Park, B.-G. Yoon, and K.-S. Soh, Phys. Rev. E **60**, 4014 (1999); H. Hong and M.Y. Choi, *ibid.* **62**, 6462 (2000).

[12] P. Jung and P. Hänggi, Phys. Rev. A **44**, 8032 (1991); L. Gammaitoni, P. Hänggi, P. Jung, and F. Marchesoni, Rev. Mod. Phys. **70**, 223 (1998).

[13] H. Sompolinsky and I. Kanter, Phys. Rev. Lett. **57**, 2861 (1986); H. Gutfreund and M. Mezard, *ibid.*. **61**, 235 (1988); M.Y. Choi, J. Choi, and K. Park, Phys. Rev. E **58**, 7761 (1998).

[14] Hu Gang, T. Ditzinger, C.Z. Ning, and H. Haken, Phys. Rev. Lett. **71**, 807 (1993); W.-J. Rappel and S.H. Strogatz, Phys. Rev. E **50**, 3249 (1994); A. Longtin, *ibid.* **55**, 868 (1997); F. Marchesoni, Phys. Lett. A **231**, 61 (1997); T. Ohira and Y. Sato, Phys. Rev. Lett. **82**, 2811 (1999); G.S. Jeon and M.Y. Choi (unpublished).